Time Domain Boundary Element Analysis of Wake Fields in Long Accelerator Structures

Kazuhiro Fujita, Hideki Kawaguchi, Robert Hampel, Wolfgang F. O. Müller, Thomas Weiland, and Satoshi Tomioka

***Abstract*—We present an explicit Time Domain Boundary Element Method (TDBEM) scheme with moving window technique for short-range wake field simulations of long accelerator structures. The proposed scheme is formulated by Kirchhoff's boundary integral equation of the scattered electromagnetic field in interior region problems. Implementation of a moving window technique in the framework of TDBEM is achieved by taking into account the causality and the retardation properties of the boundary integral equation. A parallelization algorithm for this moving window implementation is also proposed. The proposed TDBEM code with the moving window technique is applied to several practical examples of long accelerator structures. Numerical results obtained with the TDBEM code are compared with those of several finite integration codes.**

***Index Terms*—Boundary element method, moving window, parallelization, scattered fields, short-range wake field.**

I. Introduction

MANY advanced accelerator projects such as linear colliders and linac-based X-ray free electron lasers require very short and high-intensity electron bunches. As the intensity is increased, the wake field [1], which is excited by electromagnetic interactions between a beam of charged particles and its surrounding environment such as accelerating cavities, becomes stronger, and consequently it can cause energy spread and emittance growth. In order to predict such harmful effects to beam qualities, accurate knowledge of short-range wake fields of a short bunch traversing long accelerator structures such as multi-cell cavities and tapered collimators is required.

Numerical methods for wake field calculation in the time domain come in two types: the more normal type that discretizes and solves for the fields over a volume domain (subject to boundary conditions), such as is done in the Finite Integration Technique (FIT) [2] and the Finite Element Method (FEM), and the Boundary Element Method (BEM) that discretizes the charges and currents on the boundary surface, from which the fields within the enclosed domain are then obtained [3], [4]. This paper focuses on the time domain BEM analysis of the wake field. As mentioned in [3], [4], Time Domain Boundary Element Method (TDBEM) has several advantages in wake field analysis: zero dispersion in all spatial direction, conformal modeling of arbitrary 3-D geometries and treatment of a bunch of charged particles with curved trajectories. However, most of the previous TDBEM schemes have three severe drawbacks from a computational point of view: late-time numerical instabilities, heavy calculation, and large memory requirements. For the problem of numerical instabilities stable time domain schemes were recently proposed [3]–[6]. The calculation cost problems are still serious, in particular, for short bunch wake field simulations of long accelerator structures as appeared in practical accelerator designs, although a parallelization algorithm suitable for the TDBEM schemes was presented [7]. The calculation time and the required memory of the parallelized TDBEM codes become unacceptable for such large scale problems, even if a supercomputer is available.

As is well-known in the development of wake field simulation codes, it is possible to dramatically reduce the calculation costs for a time domain wake field computation by utilizing the indirect wake potential integration [8]–[11] and the moving window technique [12]. In fact, these techniques have been applied to FIT codes.

The main purpose of this paper is to introduce a moving window technique in the framework of TDBEM. In addition, the implementation of indirect wake potential integrations in TDBEM is briefly summarized. A newly developed TDBEM code with moving window technique is applied for dispersion-free time domain wake field simulations of a short bunch in long accelerator structures.

II. Scattered-Field Formulation of TDBEM

At the first part of this paper, the scattered field formulation of TDBEM is summarized for later reference.

In general, the total electromagnetic fields $(\mathbf{E}, \mathbf{B})$ are explicitly split into the bunch self-fields in free space $(\mathbf{E}_{self}, \mathbf{B}_{self})$ and the scattered fields $(\mathbf{E}_{scat}, \mathbf{B}_{scat})$:

$$\mathbf{E} = \mathbf{E}_{self} + \mathbf{E}_{scat}, \quad \mathbf{B} = \mathbf{B}_{self} + \mathbf{B}_{scat}.$$

The bunch self-fields can be then given analytically or calculated numerically. Only the scattered fields are numerically

Manuscript received March 30, 2008; revised June 02, 2008. Current version published December 04, 2008. This work was supported in part by a research grant from the Hokkaido University Clark Memorial Foundation.

K. Fujita and S. Tomioka are with the Division of Quantum Science and Engineering, Graduate School of Engineering, Hokkaido University, Kita-ku, Sapporo, 060-8628, Japan (e-mail: fujita@athena.qe.eng.hokudai.ac.jp; tom@athena.qe.eng.hokudai.ac.jp).

H. Kawaguchi is with the department of Electrical and Electronic Engineering, Muroran Institute of Technology, Muroran, 050-8585, Japan (e-mail: kawa@mmm.muroran-it.ac.jp).

R. Hampel, W. F. O. Müller and T. Weiland are with Institute fuer Theorie Electromagnetischer Felder (TEMF), Technishe Universitaet Darmstadt, D-64289, Germany.

Color versions of one or more of the figures in this paper are available at http://ieeexplore.ieee.org.

Digital Object Identifier 10.1109/TNS.2008.2002031

solved by a TDBEM scheme which is based on the retarded Kirchhoff's boundary integral equation of scattered electromagnetic fields on interior region problems. As described in [4], this scattered field formulation makes it easy to set up the initial fields on interior region problems and provides very stable time domain simulations even for small time step size.

Now we consider electromagnetic scattering problems on an interior region surrounded by the surface S of an accelerator structure. The scattered fields $\mathbf{E}_{scat}$ and $\mathbf{H}_{scat}$ can be described by the following time domain Kirchhoff's integral representations of scattered electric and magnetic field on interior problems with homogeneous material constants ε, μ [4]:

$$\begin{aligned}\mathbf{E}_{scat}(\mathbf{r},t) &= -\frac{1}{4\pi}\oint_S \Bigg\{(\mathbf{n}'\times\mathbf{E}_{scat}(\mathbf{r}',t'))\times\nabla'\frac{1}{R} \\ &\quad -\frac{1}{R}\left(\mathbf{n}'\times\frac{\partial\mathbf{E}_{scat}}{c\partial t}(\mathbf{r}',t')\right)\times\nabla' R \\ &\quad +(\mathbf{n}'\cdot\mathbf{E}_{scat}(\mathbf{r}',t'))\nabla'\frac{1}{R} \\ &\quad -\frac{1}{R}\left(\mathbf{n}'\cdot\frac{\partial\mathbf{E}_{scat}}{c\partial t}(\mathbf{r}',t')\right)\nabla' R \\ &\quad -\frac{1}{R}\left(\mathbf{n}'\times\frac{\partial\mathbf{B}_{scat}}{\partial t}(\mathbf{r}',t')\right)\Bigg\}dS', \qquad (1)\end{aligned}$$

$$\begin{aligned}\mathbf{B}_{scat}(\mathbf{r},t) &= -\frac{1}{4\pi}\oint_S \Bigg\{(\mathbf{n}'\times\mathbf{B}_{scat}(\mathbf{r}',t'))\times\nabla'\frac{1}{R} \\ &\quad -\frac{1}{R}\left(\mathbf{n}'\times\frac{\partial\mathbf{B}_{scat}}{c\partial t}(\mathbf{r}',t')\right)\times\nabla' R \\ &\quad +(\mathbf{n}'\cdot\mathbf{B}_{scat}(\mathbf{r}',t'))\nabla'\frac{1}{R} \\ &\quad -\frac{1}{R}\left(\mathbf{n}'\cdot\frac{\partial\mathbf{B}_{scat}}{c\partial t}(\mathbf{r}',t')\right)\nabla' R \\ &\quad +\frac{1}{R}\left(\mathbf{n}'\times c^{-2}\frac{\partial\mathbf{E}_{scat}}{\partial t}(\mathbf{r}',t')\right)\Bigg\}dS', \qquad (2)\end{aligned}$$

where $\mathbf{r}$ is the observation point in the interior region, $\mathbf{r}'$ is the position vector on the surface, $R=|\mathbf{r}-\mathbf{r}'|$, $c^{-2}=\varepsilon\mu$ and t' is the retarded time denoted by $t'=t-R/c$. $\mathbf{n}$ is the inward unit vector normal to the surface. The fields on the boundary S are related to the equivalent surface electric and magnetic current densities $(\mathbf{K}_s, \mathbf{M}_s)$ and charge densities (σ_s, η_s) by

$$\begin{aligned}\mathbf{n}\times\mathbf{E}_{scat} &= -\mathbf{n}\times\mathbf{E}_{self} = -\mathbf{M}_s \\ \mathbf{n}\times\mathbf{B}_{scat} &= -\mathbf{n}\times\mathbf{B}_{self}+\mu\mathbf{K} = \mu\mathbf{K}_s \\ \mathbf{n}\cdot\mathbf{E}_{scat} &= -\mathbf{n}\cdot\mathbf{E}_{self}+\sigma/\varepsilon = \sigma_s/\varepsilon \\ \mathbf{n}\cdot\mathbf{B}_{scat} &= -\mathbf{n}\cdot\mathbf{B}_{self} = \eta_s \qquad (3)\end{aligned}$$

with the real surface charge density σ and current density $\mathbf{K}$ due to the total fields. Since the equivalent surface sources $\mathbf{K}_s$, $\mathbf{M}_s$, σ_s, and η_s are related to the boundary condition of perfect conductor, the bunch self-fields indirectly excite the wake fields though $\mathbf{M}_s$ and η_s in (3).

The equations (1) and (2) can be interpreted as a mathematical expression of the so-called *surface equivalence theorem* in time domain, which states that the scattered fields in an original problem can be replaced by the fields produced by the surface equivalent current densities and charges.

This approach was named as Scattered-field Time Domain Boundary Element Method (S-TDBEM) [4].

A. Spatial and Temporal Discretizations

In this work, we adopt the magnetic field integral equation (MFIE) in time domain (2) as a basic equation. The surface S is discretized with spatial quadrilateral planar patches as boundary element and the time axis is divided by constant time step size Δt. The fields inside a boundary element are spatially expanded into the 2D curl-conforming vector basis function [13], and temporally expanded into the triangular basis function [14] (i.e. linearly-interpolated temporally). The time derivative is approximated by backward finite difference.

The evaluation of the boundary integrals in (2) should be carefully performed. In particular, for the strongly singular kernel terms of self-elements, the Cauchy principal value integration is evaluated, and by virtue of the use of planner patch it can be analytically performed [15]. For the other elements, the integrations can be numerically performed by taking into account the retarded time on the discrete time axis.

After performing this discretization procedure for (2), we finally obtain the following matrix equation:

$$[G_0]\mathbf{b}_t^n = \sum_{k=1}^{n}[G_k]\mathbf{b}_t^{n-k}+\sum_{k=0}^{n}[C_k]\mathbf{b}_n^{n-k}+\sum_{k=0}^{n}[P_k]\mathbf{e}_t^{n-k}, \qquad (4)$$

where $\mathbf{b}_t^i$, $\mathbf{b}_n^i$ and $\mathbf{e}_t^i$ denote the boundary value vectors which consist of the tangential and normal magnetic field components and the tangential electric field component on the boundary elements at time $t=i\Delta t$ $(i=0,\cdots,K)$, respectively. The coefficient matrices $[G_k]$, $[C_k]$ and $[P_k]$ are determined by the boundary integral of (2), respectively. Then, $\mathbf{b}_n^i$ and $\mathbf{e}_t^i$ are known boundary value vectors which can be calculated directly from the self-fields in (3). Therefore we finally obtain a system matrix equation as follows:

$$[G_0]\mathbf{b}_t^n = \mathbf{b}_{ext}^n+\sum_{k=1}^{n}[G_k]\mathbf{b}_t^{n-k}, \qquad (5)$$

where $\mathbf{b}_{ext}^n$ is the vector resulting from the matrix-vector multiplications of the second and the third terms in the right-hand side of (4) at a time step n. By solving the reduced matrix equation (5) at each time step, the electric surface current and charge densities induced on the boundary surface of an accelerator structure can be obtained iteratively. The matrix-vector multiplications in term of $\mathbf{b}_n^i$ and $\mathbf{e}_t^i$ over all time steps should be performed before the system matrix (5) is solved.

Once the boundary values have been obtained over all time steps, the wake fields at any position in the bounded domain can be calculated from (1) and (2).

B. Numerical Stability of System Matrix Equation

The reduced system matrix equation (5) is the starting point of discussion of time domain numerical schemes with the moving window technique in this paper. Note that the matrices $[C_k]$ and $[P_k]$ in the original matrix equation (4) do not contribute to numerical stabilities since the boundary value vectors $\mathbf{b}_n^i$ and $\mathbf{e}_t^i$ multiplied by their matrices are given, and it is not necessary to discuss the matrices $[C_k]$ and $[P_k]$ in term of the numerical stabilities of S-TDBEM. In order to consider numerical stabilities of (5), we should take into account only a set of the matrices $[G_k]$.

Many previous works [16]–[19] indicate that $c\Delta t > h_{max}$ (h_{max} is the maximum mesh size) is a stable condition in many practical cases. In fact, this tendency has been numerically validated in the Walker's eigenvalue analysis [18] for several simple cases. In this choice of time step size, a spherical surface with radius $c\Delta t$ centered at the observation point $\mathbf{r}$ contains a lot of neighbor boundary elements, or at least the closest boundary elements. Owing to this situation, the field quantities on a boundary element at the n-th time step are not independent of the ones on other adjacent boundary elements at the same time step, and thus the system matrix $[G_0]$ becomes non-diagonal. As $c\Delta t$ becomes larger, the number of boundary elements included in the $c\Delta t$ sphere increases, and therefore the number of non-zero element of $[G_0]$ increases, i.e. the system matrix equation becomes more implicit, and consequently time domain scheme becomes more stable [17]. This choice of $c\Delta t > h_{max}$ is often called *implicit scheme* while a choice of $c\Delta t < h_{min}$ (the minimum mesh size h_{min}) is called *explicit scheme*. It is well recognized that the explicit scheme is usually very unstable [17], [19]. So, most of time domain boundary element schemes (exactly saying, schemes formulated with temporally local basis function) usually employ the implicit scheme.

We have recently shown that the S-TDBEM formulation [4] is able to achieve long-time numerical stability even with very small time step size. The main reason for the stability is in reforming the scheme from the open scattering to the interior region problems. In Section VI, we will demonstrate that this approach is very stable for practical large-scale problems even in the explicit scheme.

III. Moving Window Technique in Time Domain Boundary Element Method

In order to compute the short-range wake fields of a short bunch traversing long accelerator structures at low calculation costs, a moving window technique [12] has been used in Finite Integration Technique (FIT) codes such as TBCI [20], ECHO [21], PBCI [22], and ROCOCO [23]. For the same purpose, we incorporate the concept of this technique into the TDBEM scheme.

It can be understood immediately that implicit schemes (the matrix $[G_0]$ is non-diagonal) cannot be available for the moving window technique in principle because a part of the off-diagonal elements of the matrix $[G_0]$ is corresponding to the contribution of unknown present boundary values outside the moving window, and thus the lack of boundary value information at the tail of moving window arises and it finally results in an unwanted numerical error and its accumulation. Therefore, for a moving window implementation of the TDBEM scheme, we use the explicit S-TDBEM scheme for the system matrix (5), in which the matrix $[G_0]$ is diagonal.

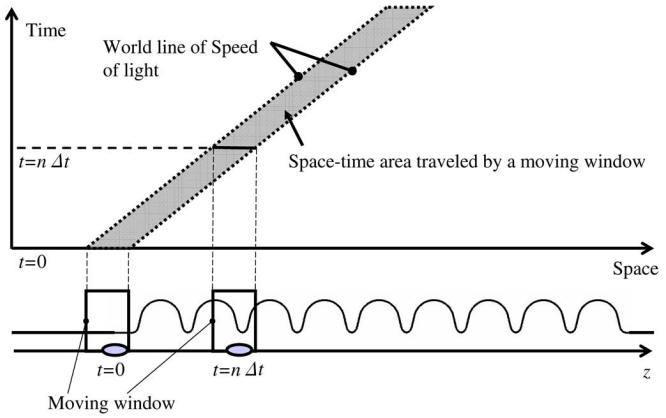

Fig. 1. Time evolution of field inside a moving window with light velocity traversing an accelerator structure on four-dimensional time space.

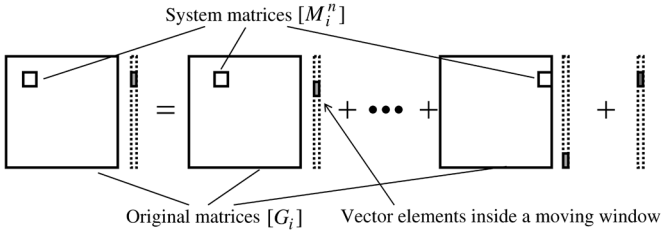

Fig. 2. System matrix equation with moving window technique.

We shall consider the explicit S-TDBEM scheme with moving window technique (S-TDBEM(w)) on a four-dimensional time-space volume which involves a bunch passing through a long multi-cell cavity as shown in Fig. 1. The basic idea of this technique is based on the following facts: (i) no field travels in front of an ultra-relativistic bunch and (ii) the fields inside the moving window with the speed of light synchronized with the bunch are not affected by any fields that happen behind the window. These two points result from causality and the assumption of rigid bunch. From this reason, we can compute only the fields over the space-time volume surrounded by the head and the end of the window (marked in Fig. 1). By taking into account this fact and (5), the S-TDBEM system matrix equation (5) can be reduced for the time domain simulation of boundary value inside the moving window, as shown in Fig. 2. The reduced matrix equation has many small system matrices $[M_i^n]$ determined by the numbers of the boundary value vector elements inside the moving window at each time step n. Accordingly, the size of a small system matrix $[M_i^n]$ depends only on the size of moving window, and does not depend on the total size of a structure. Because it is necessary for this scheme to reconstruct all of the small system matrices $[M_i^n]$ at each time step and the matrix $[M_0^n]$ is always diagonal (explicit scheme), storing the matrices $[M_i^n]$ in memory is not needed any more. Therefore, the required memory size of this scheme becomes quite smaller than that of the original TDBEM scheme. This enables us to apply the S-TDBEM(w) for practical accelerator structures as shown in Section VI.

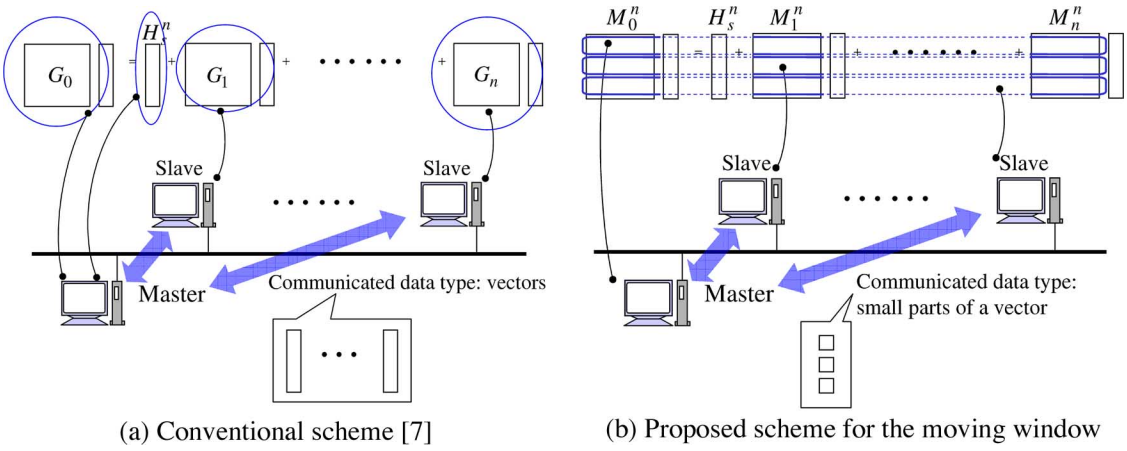

(a) Conventional scheme [7] (b) Proposed scheme for the moving window

Fig. 3. Parallelization algorithms. In (a), a set of matrix-vector multiplications is executed in each of slave CPUs, and then the resulting vectors from the multiplications are transferred to the master CPU. In (b), the reduced system matrix equation of Fig. 2 is sliced into rows, and a set of sliced multiplication parts is executed in slave CPUs. Therefore only small parts of a vector are communicated between the master CPU and slave CPU in (b). (a) Conventional scheme [7]; (b) proposed scheme for the moving window.

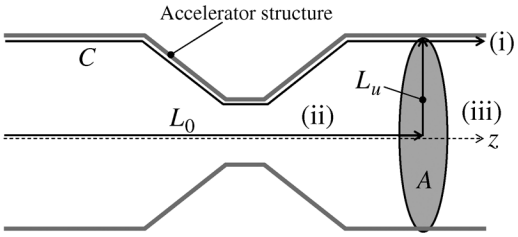

Fig. 4. Contours for wake potential calculation in TDBEM. (i) NCZ method with the contour C along the boundary cross section of a accelerator structure, (ii) NCZ modified indirect integration (line integral $L_0 + L_u$), (iii) 3D indirect integration (line integral $L_0 + 2\mathrm{D}$ Poisson's equation for pipe cross section area A).

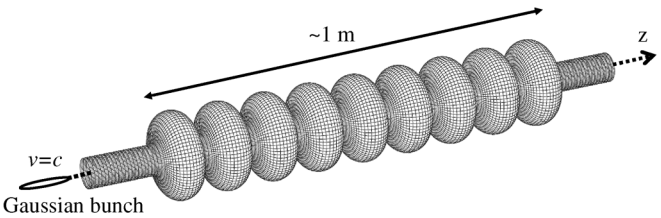

Fig. 5. Numerical model of the TESLA 9cell cavity.

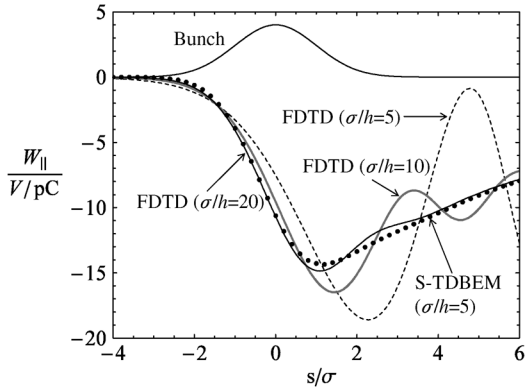

Fig. 6. Comparison of the wake potentials calculated by different methods for the TESLA 9cell cavity excited by a Gaussian bunch with $\sigma = 1$ mm.

IV. Parallelization of Moving Window Technique

As we mentioned in the previous section, the S-TDBEM(w) scheme is almost free from the problems of memory requirements. However, in the case of very long accelerator structures the calculation time becomes the most significant problem because the number of the system matrices $[M_i^n]$ still depends linearly on the total length of an accelerator structure (in realistic accelerator problems the transverse dimension of a structure is usually much smaller compared to the longitudinal size). The number of the time steps increases linearly as well. Hence, the computational effort scales quadratically with the total length. This quadratic scaling law is a main drawback of the developed moving window technique compared to the moving window implementation in FDTD because in FDTD method with moving window technique the scaling is only linear.

For this problem, we consider here a parallelization algorithm suitable for the S-TDBEM(w) scheme.

In the parallelization scheme for the conventional TDBEM in [7], since all of the system matrices are stored in memory and the matrix construction is performed once before time domain calculation, the matrix-vector multiplications in the right-hand side of system matrix equation (5) are most time-consuming and to be parallelized. Fig. 3(a) shows the parallelization of the conventional TDBEM scheme on distributed memory computing environment. A set of the system matrices is almost equally assigned and stored on the distributed memories and each CPU executes the matrix-vector multiplication of (5), and then a set of the calculation result vectors $[G_k]\mathbf{b}_t^{n-k}$ is transferred to the master CPU. After that, the master CPU executes inversion of the matrix $[G_0]$ to calculate the newest time step unknown vector $\mathbf{b}_t^n$. Finally, the newest boundary value vector $\mathbf{b}_t^n$ is broadcast to the slave CPUs for the next time step calculation.

By contrast, when the moving window technique is incorporated in the S-TDBEM scheme, since the construction of the matrices $[M_i^n]$ is performed at every time step, the calculation of the system matrices $[M_i^n]$ is the most time-consuming part in the S-TDBEM scheme and this should be parallelized. In this work the S-TDBEM(w) matrix calculation process is parallelized so that the system matrix equation is sliced into rows. Fig. 3(b) gives a schematic picture of this parallelization algorithm. This approach is also corresponding to longitudinally dividing the moving window. The advantage of the proposed parallelization

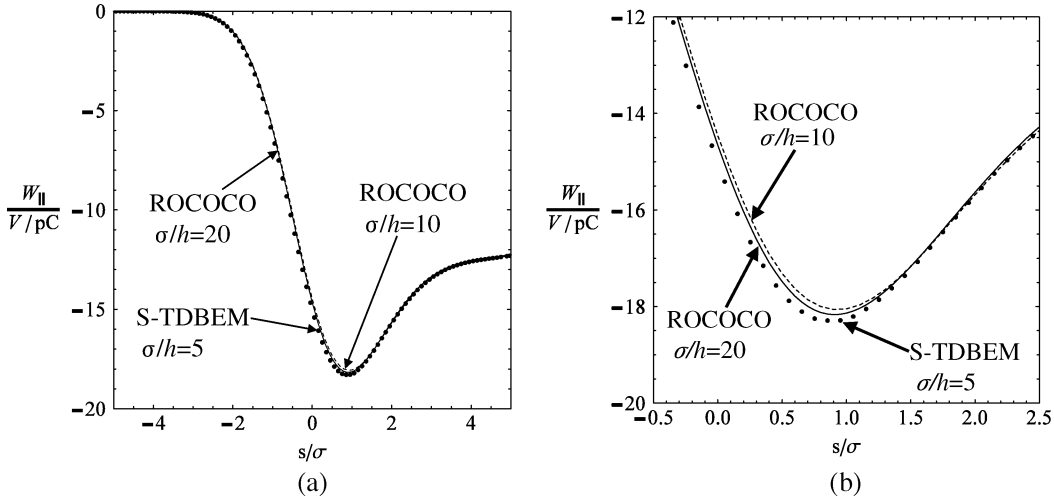

Fig. 7. Comparison of the wake potentials calculated by two dispersion-free methods for the TESLA 9cell cavity excited by a Gaussian bunch with $\sigma = 0.5$ mm. (a) $-5\sigma < s < 5\sigma$; (b) $-0.5\sigma < s < 2.5\sigma$.

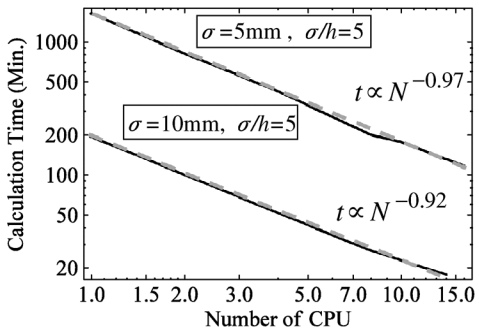

Fig. 8. Scalability of the parallelization algorithm proposed for the moving window implementation.

algorithm is that the interprocess communication between the master CPU and slave CPUs is much smaller than that of the original TDBEM scheme because only small parts of the calculated vector are transferred to the master PC.

V. Wake Potential Calculation

The wake potential [1], [24] is one of important physical quantities for quantitatively evaluating the wake field effects in the design of an accelerator. In this section we briefly summarize how to compute wake potentials in the framework of TDBEM.

The longitudinal and transverse wake potentials are defined as an normalized integral over the electromagnetic field along a test particle with unit charge following the exciting bunch $\rho(\mathbf{r}, t)$ with total charge Q traversing an accelerator structure with the same velocity $\mathbf{v}$ parallel to the z-axis and the transversal coordinates $\mathbf{r}$, at a distance s behind the bunch [24]:

$$W_{\|}(\mathbf{r}, s) = -\frac{1}{Q}\int_{-\infty}^{\infty} E_z\left(\mathbf{r}, z, t=(z+s)/v\right) dz, \tag{6}$$

$$\mathbf{W}_{\perp}(\mathbf{r}, s) = \frac{1}{Q}\int_{-\infty}^{\infty} \left(\mathbf{E}_{\perp} + \mathbf{v}\times\mathbf{B}\right)\left(\mathbf{r}, z, t=(z+s)/v\right) dz. \tag{7}$$

The transverse wake potential (7) can be obtained from the longitudinal one by applying the Panofsky-Wenzel theorem [25].

To obtain the short-range wake potential of a short bunch in long accelerator structures, direct time domain calculations of wake field are commonly made with the moving window technique and indirect integration methods [8]–[11] are often used in order to dramatically reduce the calculation time in a computer code. In the following, we shall review the implementation of indirect methods for wake potential integration.

For axis-symmetric structures, the infinite integration of wake potential can be replaced by a finite range of integration with the Napoly-Chin-Zotter (NCZ) indirect integration method [11]. Especially, selecting the integration path along the boundary surface of a structure as the path (i) shown in Fig. 4 leads to the simple calculation of the wake potentials from the total electromagnetic fields on the boundary surface, i.e., directly from the boundary values solved [3], [26]. The advantage of this path selection is that it is unnecessary to calculate the fields inside the structure. Although a modification of the NCZ indirect method [21], whose integration path is shown as the path (ii) in Fig. 4, can be also applied for S-TDBEM, additional computation of the inside fields is required. Therefore, the method (i) in Fig. 4 is quite suitable for the S-TDBEM.

For general 3-D structures, the recently developed indirect wake potential integration method [10], [11] can be also applied for the S-TDBEM. The 3-D indirect method needs a direct 1-D integration with finite length and a solution of the 2-D Poisson equation (for details, see [10], [11]) over cross-section of the outgoing beam tube as in Fig. 4. In the framework of TDBEM, the finite direct integration is made by computing the scattered fields along the beam path inside an analytical region using the field integral representations (1) and (2), and the 2-D Poisson equation can be easily solved by a standard 2-D boundary element solver.

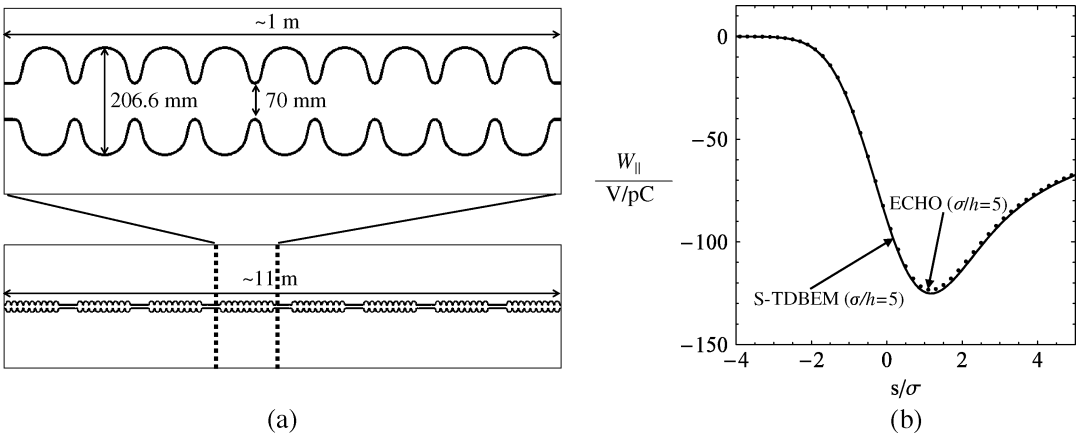

Fig. 9. Comparison of longitudinal wake potentials calculated by two different dispersion-free methods for the TESLA accelerating cryomodule excited by a Gaussian bunch with $\sigma = 1$ mm. (a) Cross section of the TESLA accelerating cryomodule which consists of eight of the TESLA 9cell cavities, (b) Longitudinal wake potential.

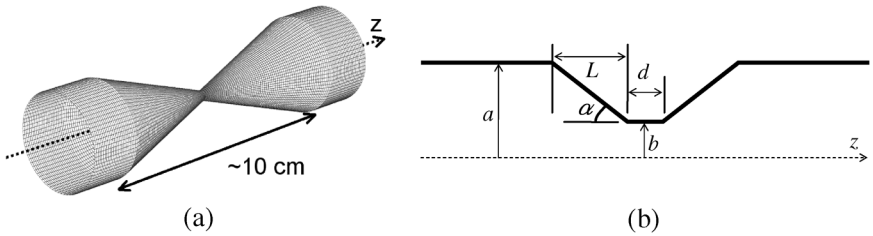

Fig. 10. Numerical model of tapered collimator and its geometry parameter. (a) 3D model; (b) cross section geometry.

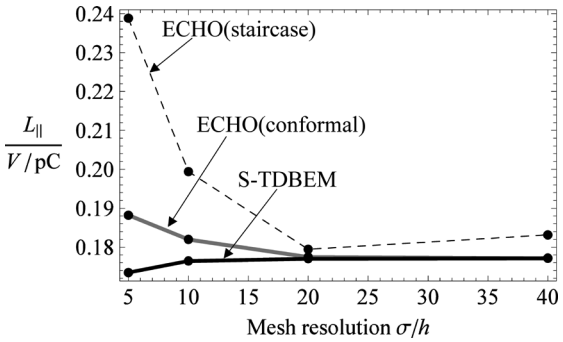

Fig. 11. Comparison of convergence properties of loss factor of a Gaussian bunch ($\sigma = 4$ mm) traversing the round tapered collimator computed by the S-TDBEM(w) and the code ECHO. The geometry parameters are: $a = 19$ mm, $b = 1.9$ mm, $d = 0$ mm, $L = 51$ mm and $\alpha = 335$ mrad in Fig. 10(b).

VI. Numerical Examples

A. TESLA 9cell Cavity

Fig. 5 shows a numerical model of the TESLA 9cell cavity [27] as an example of long accelerator structures. The total length of the cavity is about 1 m and the numerical model is assumed to be axisymmetric.

Fig. 6 shows the comparison of wake potentials of the on-axis Gaussian line bunch with RMS length $\sigma = 1$ mm calculated with the S-TDBEM(w) scheme and by a simple square mesh calculation based on a FIT scheme in cylindrical coordinates [20]. In the standard FDTD simulation oscillations are observed while in the S-TDBEM(w) simulation there is no oscillation because of the grid dispersion-free property of the S-TDBEM.

Fig. 7 shows the comparison of wake potentials computed by the proposed scheme and the code ROCOCO [23] for ultra short bunch with $\sigma = 500$ μm. The ROCOCO result for $\sigma/h = 20$ is regarded as the reference solution. Even for course mesh $\sigma/h = 5$ the proposed scheme gives more accurate result than the ROCOCO result with $\sigma/h = 10$.

In order to check the performance of this parallelization algorithm, wake field excited by a Gaussian bunch passing through the TESLA 9cell cavity is simulated for the two cases of $\sigma = 5$ mm and 10 mm. Fig. 8 demonstrates reduction rate of calculation time to the number of PCs used in the simulations. The average of the rates for the two cases is 0.95. We can confirm that the scalability is almost ideal (≈1).

B. TESLA Accelerating Cryomodule

Here we demonstrate an application of the parallelized STDBEM code to very large-scale wake field analysis. As a test example, the TESLA accelerating cryomodule which consists of eight of the TESLA 9cell cavities is simulated as in Fig. 9(a). The total length of the structure is about 11 m, the RMS length of a Gaussian bunch is 1 mm, and the grid resolution is taken to be $\sigma/h = 5$. The number of total time step is about 140000. The simulation is done with 256 CPUs on a supercomputer, the HITACHI SR-11000. The calculation time is about 19 hours.

In this case the high frequency field excited by a short bunch can propagate in the cavity, and therefore the zero grid dispersion property is very important in order to accurately compute wake potentials. As expected, the S-TDBEM(w) calculation shows no oscillation due to the numerical dispersion

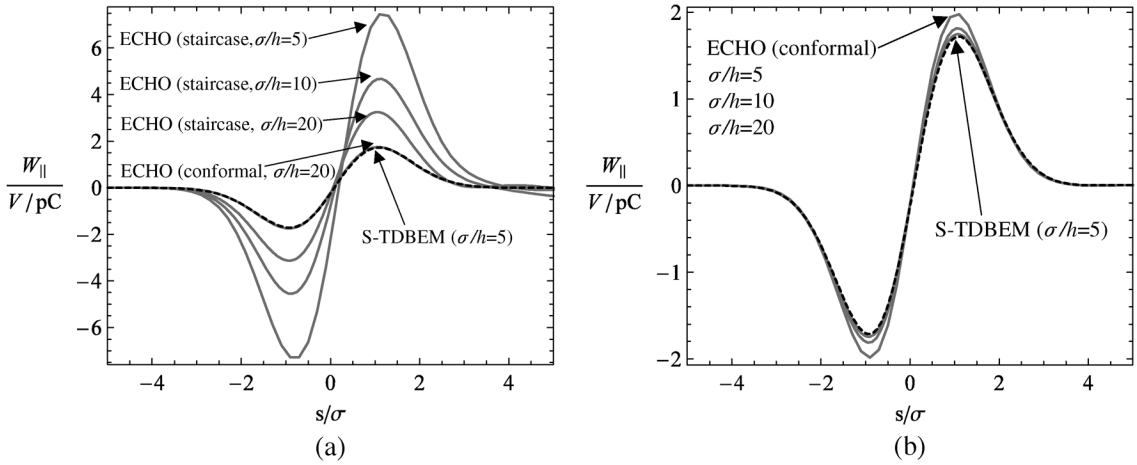

Fig. 12. Comparisons of wake potentials of a short Gaussian bunch ($\sigma = 1.2$ mm) traversing the long tapered collimator computed by the S-TDBEM(w) and the code ECHO. The geometry parameters are: $a = 19$ mm, $b = 1.9$ mm, $d = 0$ mm, and $L = 510$ mm in Fig. 10(b).

error in Fig. 9(b). We can see excellent agreement between the S-TDBEM (w) and the ECHO [21] codes.

C. Tapered Collimator

Finally we deal with an axially symmetric tapered collimator with geometry parameters $a = 19$ mm, $b = 1.9$ mm, $d = 0$ mm, $L = 51$ mm and $\alpha = 335$ mrad as shown in Fig. 10. The geometric parameters are similar to the ones of the collimator that was tested in the SLAC linac [28]. The convergence property of the proposed scheme is tested for this axisymmetric model. Fig. 11 shows the results of loss factor calculated by the S-TDBEM and the code ECHO. The loss factor is defined by

$$L_{||} = \int_{-\infty}^{\infty} \lambda(s) W_{||}(s) ds,$$

,where $\lambda(s)$ the shape distribution of a bunch. A good convergence of the S-TDBEM is demonstrated in the comparison of the computed loss factors. A Gaussian bunch with $\sigma = 4$ mm is used in this simulation. For the mesh resolution ($\sigma/h = 5$) of almost same accuracy in Fig. 11, the calculation time of our code is about 80 sec with single CPU operation in Intel(R) Core(TM)2 CPU 6400 2.13 GHz while that of ECHO(conformal) is a few sec with single CPU operation in Intel(R) Core(TM)2 CPU T5500 1.66 GHz/1.67 GHz.

Fig. 12 shows the results of longitudinal wake potential of a short Gaussian bunch ($\sigma = 1.2$ mm) traversing an axially symmetric tapered collimator with longitudinally longer dimensions ($a = 19$ mm, $b = 1.9$ mm, $d = 0$ mm, $L = 510$ mm). It is found again that the calculation by the S-TDBEM shows faster convergence than the ECHO calculations. We can conclude that even for long tapered structures the S-TDBEM works well as a conformal scheme for dispersion-free wake field calculations.

VII. Conclusion

An explicit S-TDBEM scheme with the moving window technique (S-TDBEM(w)) has been proposed for dispersion-free wake field simulations of long accelerator structures. The moving window implementation in the framework of TDBEM has been discussed, and the S-TDBEM(w) code has been applied for the TESLA 9cell cavity, the TESLA accelerating cryomodule and the tapered collimators. The numerical examples show good agreement between the numerical results calculated by the presented code and by several FIT codes such as ROCOCO and ECHO.

The simulations by the 2-D S-TDBEM(w) code are done in order to test the developed moving window technique, and only longitudinal monopole wake field calculations are shown in the numerical results. However, this is not a limitation of the developed technique, and the presented method can be applied to transverse dipole and three dimensional wake field calculations as well. A 2.5-D/general 3-D TDBEM code with this moving window technique is indeed being developed for transverse dipole and three dimensional wake field simulations.

In addition, the presented approach is available even if a bunch has curved trajectories when the bunch has very high energies and always moves inside a moving window. That is, the application of this approach is independent of the selection of wake potential integration path. Transient analysis of coherent synchrotron radiation (CSR) shielded by arbitrary 3-D vacuum chambers is another important application of S-TDBEM(w). This application will be presented in near future.

As is mentioned in Section IV, the quadratic scaling law is a main drawback of the developed technique. We are now working in development of an accelerating technique for achieving the linear scaling law of calculation time as in the moving window implementation of FDTD method.

References

[1] W. C. Chao, *Physics of Collective Beam Instabilities in High Energy Accelerators*. New York: Wiley, 1993.

[2] T. Weiland, "Time domain electromagnetic field computation with finite difference methods," *Int. J. Numer. Modeling: Electron. Networks*, vol. 9, p. 295, 1996.

[3] K. Fujita, H. Kawaguchi, I. Zagorodnov, and T. Weiland, "Time domain wake field computation with boundary element method," *IEEE Trans. Nucl. Sci.*, vol. 53, no. 2, pp. 431–439, 2006.

[4] K. Fujita, H. Kawaguchi, S. Nishiyama, S. Tomioka, T. Enoto, I. Zagorodnov, and T. Weiland, "Scattered-field time domain boundary element method and its application to transient electromagnetic field simulation in particle accelerator physics," *IEICE Trans. Electron.*, vol. E90-C, no. 2, pp. 265–274, 2007.

[5] H. Kawaguchi, "Stable time-domain boundary integral equation method for axisymmetric coupled charged-electromagnetic field problems," *IEEE Trans. Magn.*, vol. 38, no. 2, pp. 749–752, 2002.
[6] H. Kawaguchi, "Time-domain analysis of electromagnetic wave fields by boundary integral equation method," *Eng. Anal. Boundary Elements*, vol. 27, pp. 291–304, 2003.
[7] *Time Domain Techniques in Computational Electromagnetics 4*, D. Poljak and H. Kawaguchi, Eds. : WIT Press, 2004, ch. 1, pp. 1–36.
[8] T. Weiland, "Comment on wake field computation in time domain," *Nucl. Instrum. and Methods*, vol. 216, pp. 31–34, 1981.
[9] O. Napoly, Y. Chin, and B. Zotter, "A generalized method for calculating wake potentials," *Nuclear Instruments and Methods*, ser. A, vol. 344, p. 255, 1993.
[10] H. Henke and W. Bruns, "Calculation of wake potentials in general 3D structures," in *Proceedings of EPAC2006*, Edinburgh, Scotland, 2006.
[11] I. Zagorodnov, "Indirect methods for wake potential integration," *Phys. Rev. ST Accel. Beams*, vol. 9, p. 102002, 2006.
[12] K. Bane and T. Weiland, "Wake force computation in the time domain for long structures," in *Proc. 12th Int. Conf. on High Energy Accel.*, Chicago, IL, 1983, p. 314.
[13] J. Jin, *The Finite Element Method in Electromagnetics 2nd edition*. New York: John Wily &Sons, Inc, 2002.
[14] S. M. Rao and D. R. Wilton, "Transient scattering by conducting surfaces of arbitrary shape," *IEEE Trans. Antennas Propagat.*, vol. 39, no. 1, pp. 56–61, 1991.
[15] N. Morita, N. Kumagai, and J. R. Mautz, *Integral Equation Methods for Electromagnetics*. Norwood, MA: Artech House, 1990.
[16] H. Kawaguchi and T. Homma, "Consideration on numerical instability of Dirichlet Gauge BEM," *IEEE Trans. Magnetics*, vol. 32, no. 3, pp. 914–917, 1996.
[17] M. J. Bluck and S. P. Walker, "Time-domain BIE analysis of large three-dimensional electromagnetic scattering problems," *IEEE Trans. Antennas Propagat.*, vol. 45, no. 5, 1997.
[18] S. P. Walker, M. J. Bluck, and I. Chatzis, "The stability of integral equation time domain computations for three-dimensional scattering; similarities and differences between electrodynamic and elastrodynamic computations," *Int. J. Numer. Model.*, vol. 15, pp. 459–474, 2002.
[19] B. H. Jung and T. K. Sarkar, "Time-domain CFIE for the analysis of transient scattering from arbitrarily shaped 3D conducting objects," *Microwave Opt. Technol. Lett.*, vol. 34, no. 4, pp. 289–296, 2002.
[20] T. Weiland, "Transverse beam cavity interaction-part I: Short range forces," *Nucl. Instrum. and Methods*, vol. 212, pp. 13–34, 1983.
[21] I. Zagorodnov, R. Schuhmann, and T. Weiland, "Long-time numerical computation of electromagnetic fields in the vicinity of a relativistic source," *J. Comput. Phys.*, vol. 191, pp. 525–541, 2003.
[22] E. Gjonaj *et al.*, "Large scale parallel wake field computation for 3D-accelerator structures with the PBCI code," in *Proc. ICAP 2006*, Chamonix, France, pp. 29–34.
[23] R. Hamplel, W. F. O. Muller, and T. Weiland, "ROCOCO-A zero dispersion algorithm for calculating wake potentials," in *Proc. ICAP 2006*, Chamonix, France, pp. 144–147.
[24] B. W. Zotter and S. A. Kheifets, *Impedances and Wakes in High-Energy Particle Accelerators*. , Singapore: World Scientific, 1998.
[25] W. K. H. Panofsky and W. A. Wenzel, "Some considerations concerning the transverse deflection of charged particles in radio-frequency fields," *Rev. Sci. Instr.*, vol. 27, p. 947, 1956.
[26] K. Fujita and H. Kawaguchi, "Particle accelerator wake potential calculation by time domain boundary element method," *Computational Engineering I, JASCOME*, pp. 101–108, 2004.
[27] TESLA Technical Design Report Hamburg, Germany, DESY 2001-011, 2001, Part II.
[28] I. Zagordnov, T. Weiland, and K. Bane, SLAC-PUB-9985, 2003.